

Lawrence Berkeley National Laboratory

Lawrence Berkeley National Laboratory

Title

MAS NMR Study of the Metastable Solid Solutions Found in the LiFePO₄/FePO₄ System

Permalink

<https://escholarship.org/uc/item/3cf8q8pz>

Author

Cabana, Jordi

Publication Date

2009-11-10

Submitted for publication as part of the special issue on The Materials Chemistry of
Energy Conversion

MAS NMR Study of the Metastable Solid Solutions Found in the $\text{LiFePO}_4/\text{FePO}_4$ System

*Jordi Cabana,^{†, ‡} Junichi Shirakawa,[†] Guoying Chen,[‡] Thomas J. Richardson,[‡] Clare P.
Grey^{†, *}*

[†] Chemistry Department, Stony Brook University, NY 11794-3400, USA.

[‡] Environmental Energy Technologies Division, Lawrence Berkeley National Laboratory,
Berkeley, CA 94720, USA

*corresponding author: cgrey@notes.cc.sunysb.edu

RECEIVED DATE (to be automatically inserted)

Abstract

$^6, ^7\text{Li}$ and ^{31}P NMR experiments were conducted on a series of single- or two-phase samples in the $\text{LiFePO}_4\text{-FePO}_4$ system with different overall lithium contents, and containing the two end-members and/or two metastable solid solution phases, $\text{Li}_{0.6}\text{FePO}_4$ or $\text{Li}_{0.34}\text{FePO}_4$. These experiments were carried out at different temperatures in order to search for vacancy/charge ordering and ion/electron mobility in the metastable phases. Evidence for $\text{Li}^+\text{-Fe}^{2+}$ interactions was observed for both $\text{Li}_{0.6}\text{FePO}_4$ and $\text{Li}_{0.34}\text{FePO}_4$. The strength of this interaction leads to the formation of LiFePO_4 -like clusters in the latter, as shown by the room temperature data. Different motional processes are proposed to exist as the temperature is increased and various scenarios are discussed. While concerted lithium-electron hopping and/or correlations explains the data below 125°C , evidence for some uncorrelated motion is found at higher temperatures, together with the onset of phase mixing.

Introduction

Lithium-ion batteries have played a central role in the rapid development, in recent years, of portable digital and wireless technology. Such success has triggered further efforts to utilize them as components in other applications with an even larger impact on society, which include electric vehicles and onsite storage for energy from renewable sources. However, several challenges need to be met before these expectations can be realized, as current commercial Li-ion batteries currently do not meet the cost, energy and power density requirements of these devices^{1, 2} Lithium iron phosphate, LiFePO_4 , a phospho-olivine first proposed for use as a positive electrode by Padhi *et al.*,³ has become a key player in the path toward these technical achievements, and now stands as a strong candidate to be the positive electrode of choice in the next generation of batteries designed for transportation^{4, 5} because of its low cost, low toxicity, and excellent thermal stability.⁶ Upon delithiation, LiFePO_4 is converted to FePO_4 via a first-order transition, a reaction that occurs at about 3.4 V vs. Li^+/Li^0 and corresponds to a theoretical capacity of 170 mAh/g. Delacourt *et al.*⁷ demonstrated the possibility of transforming of two-phase mixtures of these two end members to single-phase Li_xFePO_4 solid solutions at elevated temperatures. The cooling of solid solution samples with $x > 0.45$ has been reported by several groups to result in the formation of a metastable intermediate phase, formulated as $\text{Li}_{0.6}\text{FePO}_4$, mixed with different proportions of LiFePO_4 and FePO_4 .⁸⁻¹⁰ Mössbauer and phonon densities of states studies indicate that this phase shows structural disorder at high temperatures.¹¹⁻¹⁴ Rietveld refinements of neutron diffraction patterns of quenched samples containing this phase suggest that it remains disordered at room temperature, with shorter average Fe-O bonds and longer

average M1-O lengths (M1 refers to Li when present, and to the center of the Li site when it is vacant) compared to LiFePO_4 .⁸ Recently, another metastable line phase, $\text{Li}_{0.34}\text{FePO}_4$, was shown to coexist with FePO_4 in slowly cooled crystals with lower lithium content.^{10, 14} Li_xFePO_4 phases, with x between 0.3 and 0.8 have also been prepared by quenching high temperature solid-solution samples.^{10, 14}

In highly crystalline samples, the line phases $\text{Li}_{0.6}\text{FePO}_4$ and $\text{Li}_{0.34}\text{FePO}_4$ may coexist with the end members for long periods of time at room temperature. Transmission electron microscopy (TEM) and selected area electron diffraction (SAED) studies showed that the interfaces are in the (010) plane, which suggests that phase separation of the high temperature solid solutions proceeds by migration of lithium ions within the tunnels aligned with the b -axis, thereby producing stacked layers of different compositions with phase boundaries in the ac plane.¹⁵ In contrast, in the partially oxidized but unheated two-phase $x\text{LiFePO}_4/(1-x)\text{FePO}_4$ crystals, the end members are located in stripes alternating along the a direction with phase boundaries in the bc plane.¹⁵

Magic angle spinning nuclear magnetic resonance (MAS NMR) has proven to be a very useful technique to study short range ordering schemes that are not detectable by diffraction techniques in positive electrode materials¹⁶ such as LiMn_2O_4 -¹⁷⁻²¹ and LiMO_2 -type ($M=\text{Mn}^{22, 23}$, Co^{24} and/or Ni^{25-32}) phases, both in pristine and in charged/discharged samples. When experiments at different temperatures are combined, additional information regarding the diffusion of lithium and/or electron hopping can also be obtained.^{25, 27, 33-38} Since the intermediate Li_xFePO_4 phases necessarily contain lithium vacancies and mixed $\text{Fe}^{3+}/\text{Fe}^{2+}$ states,^{6, 7} ^6Li and ^{31}P NMR experiments were conducted in

this study in order to search for vacancy/charge ordering and enhanced ion/electron mobility in these phases. This study focuses on a series of samples with different overall lithium contents that comprise either a combination of the two end-member compounds (LiFePO_4 and FePO_4), a single (metastable) phase derived by quenching from high temperature, or multi-phase composite (laminar) crystals formed by slow-cooling. Through a combination of room and high (up to 250°C) temperature MAS NMR experiments we show the existence of different degrees of Li^+ - Fe^{2+} correlations which are thought to be behind charge ordering, motional processes and phase stability of the metastable solid solution phases. Several mobility scenarios are also discussed.

Experimental

Synthesis. LiFePO_4 crystals measuring $2 \times 0.2 \times 4 \mu\text{m}$ along the *a*, *b*, and *c*-axes, respectively, were synthesized using the hydrothermal method described previously.¹⁵ FeSO_4 (99%, Aldrich) and H_3PO_4 (85%, J. T. Baker) were mixed in deoxygenated and deionized water, and a LiOH (Spectrum) solution was added slowly to the mixture to give an overall Fe:P:Li ratio of 1:1:3. After stirring under helium gas for about 5 min, the reaction mixture was transferred to a Parr reactor, which was purged with helium and held at 220°C for 3 h. On cooling to room temperature, the off-white precipitate was filtered, washed with deionized water, and dried at 60°C under vacuum for 24 h. Delithiated crystals were obtained by stirring in a 0.05 M solution of bromine in acetonitrile (Sigma-Aldrich) for 1 h, by adjusting the molar ratio to achieve the desired stoichiometry. The two-phase mixtures thus obtained were placed in a tube furnace purged with flowing argon and heated in steps to 200, 250, 300 and 375°C at a rate of 5

°C/min, followed by holding at each temperature for 2 h. The samples were then sequentially cooled at the same rate from 375 to 250, 200, 150 and 100 °C by holding at each temperature for 2 h before reaching room temperature. In contrast, the quenched samples were prepared by quickly cooling the sealed sample container between two metal blocks.

X-ray diffraction. X-ray diffraction (XRD) patterns were acquired in reflection mode using a Panalytical Xpert Pro diffractometer equipped with monochromatized Cu K α radiation ($\lambda=1.5406$ Å). The scan rate was 0.0025°/s from 10 to 70° 2 θ in 0.01° steps. The phase ratios in $x\text{LiFePO}_4/(1-x)\text{FePO}_4$ two-phase mixtures and in the cooled solid solution crystals were determined by refinement of the XRD data with the Riqas Rietveld refinement software (MDI).

Nuclear magnetic resonance spectroscopy. Room temperature ^6Li , ^7Li and ^{31}P magic angle spinning nuclear magnetic resonance (MAS NMR) experiments were performed with a double-resonance 1.8 mm probe, built by A. Samoson and co-workers (KBFI, Tallinn, Estonia), on a CMX-200 spectrometer using a magnetic field of 4.7 T, at a spinning frequency of 38 kHz and using a rotor-synchronized spin-echo sequence ($\pi/2$ - τ - π - τ -aq). The ^7Li spectra were collected at an operating frequency of 77.71 MHz, with a 2.75 μs $\pi/2$ pulse width and an acquisition delay of 0.2 s, whereas the ^6Li MAS NMR measurements were conducted at an operating frequency of 29.42 MHz, with a 4.5 μs $\pi/2$ pulse width and an acquisition delay of 0.2 s. In both cases, 1 M LiCl (at 0 ppm) was used as an external reference. In the case of the ^{31}P data, the observed signals were very broad and, thus, the whole spectrum could not be excited simultaneously. Instead, separate spectra were acquired as a function of irradiation frequency, starting at a carrier

frequency of 80.94 MHz, which corresponds to the Larmor frequency of the reference (a solution of H_3PO_4 , set at 0 ppm). The carrier frequency was moved in steps of 650 kHz and the resulting spectra were normalized to the same scan number and mathematically added to yield the quantitative, full spectrum corresponding to each sample. For all frequencies, the $\pi/2$ pulse width was 3.0 μs and the delay time was set at 0.1 s.

Variable temperature ^7Li and ^{31}P MAS NMR experiments were carried out with an Oxford magnet operating at a magnetic field of 4.7 T, along with an INFINITY-console, by using a Chemagnetics variable temperature stack and a Chemagnetics double resonance 3.2 mm probe. The rest of the experimental parameters used for the acquisition of the data were the same as used for the room temperature experiments.

Results

XRD phase analysis. Chemical oxidation of LiFePO_4 crystals produced delithiated samples consisting of two-phase mixtures of $x\text{LiFePO}_4$ and $(1-x)\text{FePO}_4$. The samples were characterized by XRD, HRTEM, X-ray absorption spectroscopy (XAS), Fourier transform infrared (FTIR) and Raman spectroscopy, and were found to be free of amorphous materials and other impurity phases.^{10, 15, 39} When partially oxidized crystals ($x = 0.14, 0.54, \text{ and } 0.74$) were heated in an inert atmosphere, single-phase, solid solutions formed at temperatures ranging from 250-300°C, the actual temperature being systematically lower for lithium contents close to 0.60. Slow cooling resulted in demixing and precipitation of intermediate phases, with the phase compositions and their relative ratios in the end products depending on the total amount of Li present.¹⁰ Figure 1a shows the XRD patterns of the end members along with those of the slow cooled

samples, which will be referred to as SC0.14, SC0.54 and SC0.74 throughout the text for convenience. For instance, SC0.14 denotes the slow cooled sample with overall Li content $x = 0.14$ (table 1). The 211/020 peak intensities are compared to show the relative amounts of the intermediate phases ($\text{Li}_{0.6}\text{FePO}_4$ and $\text{Li}_{0.34}\text{FePO}_4$) and the end members in each sample. Rietveld refinement of the entire patterns gave the compositions shown in Table 1. When a solid solution sample with $x = 0.54$ was quenched (henceforth referred to as Q0.54) rather than being slowly cooled, the single phase, i.e., $\text{Li}_{0.54}\text{FePO}_4$, could be preserved at room temperature, as shown in Fig. 1b. This quenched sample slowly disproportionated to the end members when aged at room temperature, containing significant amounts of both LiFePO_4 and FePO_4 after 5 months (Figure 1b). The solid solution phase in the sample maintained a Li content of $x = 0.54$, during this time. Other single phase solid solutions were also obtained when two phase mixtures with $x = 0.48$ and $x = 0.74$ were heated to $375\text{ }^\circ\text{C}$ and then quenched. These, however, quickly demixed to the end members at room temperature. Thus, certain intermediate compositions close to $\text{Li}_{0.6}\text{FePO}_4$, the eutectoid point in the phase diagram,⁹ appear to be more stable upon quenching than others.

Room temperature NMR. In general, MAS NMR spectra are composed of an envelope comprising an isotropic resonance and spinning sidebands. In compounds containing paramagnetic ions (i.e., $\text{Fe}^{2+}/\text{Fe}^{3+}$, in this case), the shift is dominated by Fermi contact interactions between the lithium ions and these paramagnets, which result in the transfer of unpaired electron spin density from the latter to the former, through the ligand anions (oxide, in this case). The spinning sidebands arise from the partial averaging by MAS of the large dipolar interaction between the Li nuclei and the magnetic moments of the

paramagnetic centers.¹⁶ In LiFePO_4 , lithium ions occupy a single, centrosymmetric, distorted octahedral (M1) site surrounded by three pairs of oxide ions and three pairs of Fe^{2+} ions (Fig. 2a).⁴⁰ The cations in one of the latter pairs are connected through two oxide ions, leading to a total of four Fe-O-Li contacts with angles near 90° (table 2). One of these oxide ions also links Li to iron ions of another pair (for a total of two contacts at 111.0°), while the third pair is linked through single oxide ions at 121.5° , also leading to a total of two Fe-O-Li contacts. The average coordination around the vacant Li site in Li_xFePO_4 is only slightly modified.⁸ The ^7Li resonance at -56 ppm observed in the MAS NMR spectrum of pristine LiFePO_4 is assigned to this crystallographic site (see Figure S1 in the Supporting Information), in accordance with previous results.⁴¹⁻⁴⁴

Figure 3 shows the isotropic resonance region of the ^6Li MAS NMR spectra of SC0.14, SC0.54, SC0.74, and Q0.54 together with that of a non-heat treated two-phase mixture of 62% LiFePO_4 and 38% FePO_4 ($x = 0.62$, henceforth referred to as NHT0.62). Despite the considerable breadth of all the isotropic resonances, differences in their centers of gravity and lineshape can be observed between samples. Spectral deconvolution (red and green lines in Figure 3) revealed that, while the signals from Q0.54, SC0.54 and NHT0.62 could be fit with one broad resonance, those from SC0.14 and SC0.74 are asymmetric and, therefore, better fit by using two peaks. Equally good fits can be performed by using more peaks, but in the absence of any further data, we have chosen to use the simplest model possible. That only one signal is seen for NHT0.62 is not surprising, because one of the phases (FePO_4) contains no (or, at most, a negligible amount of) Li. Similarly, the single resonance in the spectrum of SC0.54 is assigned to $\text{Li}_{0.6}\text{FePO}_4$, the FePO_4 component (comprising 10% of the sample) again being

undetectable by Li NMR. Q0.54 consists of single-phase $\text{Li}_{0.54}\text{FePO}_4$, as stated above. Shifts of *ca.* -64 ppm for LiFePO_4 , *ca.* -26 ppm for $\text{Li}_{0.6}\text{FePO}_4$ and *ca.* -20 ppm for $\text{Li}_{0.54}\text{FePO}_4$ are observed, the gradual shift to higher frequency with decreasing Li content being consistent with the higher Fe^{3+} contents.^{38,43}

Previously reported neutron diffraction data for $\text{Li}_{0.6}\text{FePO}_4$ at room temperature⁸ suggested the existence of a single environment for lithium, which, in principle, is consistent with the single resonance observed in the ^6Li MAS NMR spectrum. However, this phase contains iron in a mixed oxidation state, $\text{Fe}^{2+}/\text{Fe}^{3+}$. In the absence of rapid lithium motion and/or electron hopping, a random distribution of these two ions in the framework will lead to a series of local lithium environments with varying proportions of Fe^{2+} and Fe^{3+} in their first coordination spheres. Such short-range effects are not observable with diffraction techniques, but NMR should be very sensitive to them; a concomitant distribution of resonances would, therefore, be expected. The observed resonances are broad, and so it could be possible that the different resonances are not resolved. However, a noticeable increase in broadening between the $\text{Li}_{0.6}\text{FePO}_4$ and LiFePO_4 resonance (for example, in the spectrum of the NHT0.62 sample) would consequently be expected. This is not observed experimentally, as the widths of both resonances are approx. 4 kHz. Two different situations, both compatible with the earlier refinement results, can be envisaged to explain the single resonance observed for $\text{Li}_{0.6}\text{FePO}_4$. The first assumes the existence of fast electron hopping and/or lithium motion, which could produce, if faster than the NMR timescale (i.e., if occurring with a hop frequency greater than the frequency separation between the different resonances), an average signal for all the existing individual environments with their various $\text{Fe}^{2+}/\text{Fe}^{3+}$

contents. A second mechanism must be present if there is negligible electronic and/or ionic motion. In this case, clusters around Li must be present that contain a discrete numbers of Fe^{2+} and Fe^{3+} ions. These clusters must be distributed randomly throughout the crystal framework, or be present in domains with small coherence lengths, since no long-range ordering has so far been detectable by diffraction techniques. These two suggestions will be explored in more detail below.

According to XRD, SC0.74 is a mixture of 64 % $\text{Li}_{0.6}\text{FePO}_4$ and 36 % LiFePO_4 . This is consistent with the presence of two peaks with shifts of -22 and -61 ppm, with integrated intensities that result in a phase fraction of *ca.* 70% $\text{Li}_{0.6}\text{FePO}_4$ and 30% LiFePO_4 . Three peaks at 218, -1 and -63 ppm were used to fit the spectrum of SC0.14. Unfortunately, the low lithium content, combined with the low natural abundance of ^6Li (*ca.* 7.6%), leads to a spectrum with a poorer signal-to-noise ratio than observed for the other samples, even at long acquisition times. Hence, the possibility that an additional resonance is present under the broad peak centered at -25 ppm cannot completely be excluded. The extremely peak at 218 ppm in the ^6Li spectrum is assigned to an unknown impurity not detected by XRD, also found in the starting LiFePO_4 batch used to prepare this sample. The large positive hyperfine shift suggests that that this impurity contains Fe^{3+} . Since the intensity of this resonance corresponds to less than 4% of the total Li content, which is itself small, the concentration of this impurity is extremely small. Since SC0.14 also contains $\text{Li}_{0.34}\text{FePO}_4$ and FePO_4 , the -1 and -63 ppm resonances likely correspond to environments in the former lithiated phase. The peak at -63 ppm is assigned to lithium ions in an environment that is very close to that of LiFePO_4 and, hence, mostly or exclusively contains Fe^{2+} in their coordination spheres. The shift of the

-1 ppm resonance indicates that lithium ions in this type of environment are surrounded by some Fe^{3+} ions. Since even more positive shifts (up to 70 ppm) have recently been observed in olivine-type samples containing more than 50% Fe^{3+} ,⁴³ this new environment must still be surrounded by significant number of Fe^{2+} ions. The appearance of LiFePO_4 -like environments in a sample with so little lithium (and thus, Fe^{2+}) strongly suggests the existence of Li^+ - Fe^{2+} clustering in the structure of $\text{Li}_{0.34}\text{FePO}_4$. Hypothetically, these clusters would be formed by a core (or region) of Li ions only surrounded by Fe^{2+} (resonance at -63 ppm), and a shell of Li ions in environments with intermediate $\text{Fe}^{2+}/\text{Fe}^{3+}$, corresponding to the observed resonance at -1 ppm (and any possible unresolved shoulders). Such clustering would help to explain the deviations from Vegard's law of the cell parameters of $\text{Li}_{0.34}\text{FePO}_4$, which are closer to those of LiFePO_4 than expected;¹⁰ extended Li^+ - Fe^{2+} clusters may have a stronger steric pillaring effect than in the case of random occupancy of Li^+ and Fe^{2+} in the framework of this phase, and the presence of these relatively incompressible domains would result in a larger measured unit cell. FePO_4 -like (i.e., Li-free) environments must be more abundant than predicted if $\text{Fe}^{2+}/\text{Fe}^{3+}$ were randomly distributed in the network, since the major Li environments are nearby Fe^{2+} only. This conclusion is consistent with recent Fourier transform infrared (FTIR) results,³⁹ where the spectrum of $\text{Li}_{0.6}\text{FePO}_4$ showed peaks with frequencies intermediate to those of the end members, suggesting an averaged $\text{Fe}^{2+}/\text{Fe}^{3+}$ environment. In contrast, the IR spectrum of $\text{Li}_{0.34}\text{FePO}_4$ resembled that of FePO_4 , consistent with the dominance of Fe^{3+} environments in that phase. The existence of two resolvable resonances in the ^6Li MAS NMR spectrum of $\text{Li}_{0.34}\text{FePO}_4$ indicates the lack of environment averaging (on the NMR timescale) by electron or ion hopping in this phase.

Further information concerning the local structure of these intermediate phases was obtained from ^{31}P MAS NMR data. Figure 4 shows the spectra of SC0.14 and SC0.54, together with those of LiFePO_4 and FePO_4 . The hyperfine shifts for phosphorus in paramagnetic materials cover a very large range which can span to more than 15000 ppm,⁴⁵ and, thus, they are very sensitive to both oxidation state and geometrical changes in the environment of the cation. The resonances observed for LiFePO_4 and FePO_4 appear at 3750 and 5770 ppm, respectively, consistent with other reports.^{45, 46} The coordination around phosphorus in LiFePO_4 and FePO_4 is shown in Figure 2b. There are five near neighbor Fe ions, one (labeled “a”) connected through two identical oxide ions (O3), so that the PO_4 tetrahedron shares an edge with the distorted FeO_6 octahedron. The Fe-O(3)-P angles are both near 90° (Table 3). These O3 ions also provide a link to a pair of iron ions (b) at a much larger angle, over 120° , while two more Fe ions (c and d) are bonded through O1 and O2, respectively, also at large angles. Thus, the total number of Fe-O-P contacts is six. The geometry of the compact and rigid PO_4 unit is barely affected by conversion of LiFePO_4 to FePO_4 , but the Fe-O distances are substantially contracted, as expected from the smaller ionic radius of Fe^{3+} ,⁴⁷ and the Fe-O-P angles for Fe(c) and (d) are increased. The dramatic change in the ^{31}P shift is mainly ascribed to the presence of Fe^{3+} (with 5 unpaired electrons) instead of Fe^{2+} (4 unpaired electrons) in the latter, and the increased covalency (and thus spin-density transfer) in Fe^{3+} -O vs. Fe^{2+} -O bonds. Therefore, as in the case of lithium, the more highly charged iron cation induces a more positive NMR shift; the effect is, however, much more dramatic, reflecting the increased covalency (and bond-order) of a phosphate P-O vs. a Li-O bond.⁴⁶

At least three different isotropic resonances were found in the spectrum of SC0.54, at 3070, 4930 (the lineshape of this resonance suggesting that there may be more than one overlapping peak) and 5800 ppm. The two lower frequency resonances are assigned to environments in the $\text{Li}_{0.6}\text{FePO}_4$ phase. At first glance, the 5800 ppm peak appears to account for too large a proportion of the total intensity of the spectrum to be solely due to the presence of 10% FePO_4 in the sample, as found by XRD. However, given that the signal due to FePO_4 is both sharper and is associated with a longer T_2 than the resonance of LiFePO_4 ,⁴⁸ the assignment of the 5800 ppm to the delithiated end member would, in principle, seem reasonable. Nonetheless, we cannot exclude the possibility that some of the signal originates from $\text{Li}_{0.6}\text{FePO}_4$. Thus, there are *at least* two different phosphorus environments in this phase, resulting from different numbers and types of interactions with Fe^{2+} and Fe^{3+} . Based on the shifts found for LiFePO_4 and FePO_4 , the peak(s) at 4930 ppm is (are) assigned to a phosphorus environment(s) surrounded by both Fe^{2+} and Fe^{3+} ions, with a slightly larger amount of nearby Fe^{3+} ions, given its closer proximity to the FePO_4 signal. The assignment of the signal at 3070 ppm is less straightforward, as it falls outside the range defined by the all- Fe^{3+} and all- Fe^{2+} olivine structures. Based on its frequency, it is assigned to a Fe^{2+} -only phosphorus environment. The decrease in shift with respect to that of the lithium ions in LiFePO_4 suggests a modification of the Fe^{2+} -O-P interaction. One cause could be geometric; the presence of lithium vacancies in the structure (Table 3) could induce changes in the Fe-O-P bond angles, which, in turn, affect the efficiency of the spin density transfer from Fe to P, through O. The contacts at a close-to- 90° interaction produce stronger $d_{\text{Fe}-\text{pO}-\text{sLi}}$ orbital overlaps than those around 120° ,³⁴ so the increase from 94° to 96° seen for the

solid solution phase leads to weaker transfer and a smaller observed shift than seen for environments in LiFePO_4 . Another factor that should be taken into account is the possible effect of an overall change in the P-O bonding in the compound due to the introduction of holes in the O 2p band when lithium is removed, as recently suggested based on electron energy loss and X-ray absorption/emission spectroscopy, coupled with DFT calculations.^{49, 50} Such changes in P-O bonding are also thought to be at the origin of the shift to higher energy of the white lines in the P K-edge XAS spectrum of FePO_4 when compared to LiFePO_4 .⁵¹

The existence of a limited number of resonances, and, hence, the absence of a single average environment in the ^{31}P spectrum for $\text{Li}_{0.6}\text{FePO}_4$ appears to conflict with the electronic/Li hopping scenario proposed as one model to explain the ^6Li MAS NMR data above. However, the resonance frequency separation (in units of Hz) is much larger for the ^{31}P than for the ^6Li spectra, meaning that a faster hopping rate will be required to result in coalescence of the ^{31}P resonances. Therefore, such a scenario cannot be excluded. Nonetheless, the fact that individual resonances can, to some degree, be resolved, and the relatively low intensity in the 4000-4500 ppm region, suggests that some short range ordering (clustering), with favored phosphorus environments, does exist. A random arrangement of $\text{Fe}^{2+/3+}$ would lead to a very complex spectrum due to the variety of $\text{Fe}^{2+}/\text{Fe}^{3+}$ permutations in the different positions (with different angles) around the phosphorus environment (Fig. 2b), with increased intensity around 4000-4500 ppm, due to the higher probability of finding environments with both Fe^{2+} and Fe^{3+} ions. Unfortunately, the resolution obtained even at very high spinning speeds (38 kHz) does not permit further quantification of the number of environments and, consequently, the

proposal of possible ordering schemes at this time. The ^{31}P MAS NMR spectrum of Q0.54 (i.e., $\text{Li}_{0.54}\text{FePO}_4$) is very similar to that of SC0.54 (Fig. 5), except for a somewhat larger relative intensity at frequencies above 5000 ppm for the latter, which is ascribed to the presence of FePO_4 in the sample. This confirms that the phases $\text{Li}_{0.54}\text{FePO}_4$ and $\text{Li}_{0.6}\text{FePO}_4$ are structurally very similar, and that at least part of the intensity above 5000 ppm observed in the fast spinning spectrum of $x = 0.54$ in Figure 4 is due to FePO_4 -like environments in both samples. Finally, the ^{31}P MAS NMR spectrum of SC0.14 is dominated by a resonance at 5790 ppm (Fig. 4), consistent with the dominance of the FePO_4 phase (59% from XRD, Table1). The small, broad, isotropic peak at 3640 ppm (see zoom-in in figure 4), is assigned to Fe^{2+} -rich, LiFePO_4 -like phosphorus environments in $\text{Li}_{0.34}\text{FePO}_4$, consistent with the corresponding ^6Li NMR shift at -62 ppm and the proposed existence of Li^+ - Fe^{2+} clustering. As described above, this clustering model results in a phase that is dominated by Li-free regions (or larger clusters), which contribute to the intensity of the FePO_4 -like peak at 5790. In addition, such a model would also predict (at least) one additional environment, at the interface between the Li^+ - Fe^{2+} clusters and larger Li^+ - Fe^{3+} domains (where Li^+ is a Li^+ vacancy), that contains both Fe^{2+} and Fe^{3+} ions, and would be associated with a ^{31}P shift above 4000 ppm. No such peak(s) could be clearly resolved, most likely because of its (their) low predicted intensity (similar to what is observed for the corresponding ^6Li MAS NMR spectrum). However, the “ LiFePO_4 ”-like resonances are broad and there appear to be other buried under the large sideband manifolds of the 5790 and 3640 ppm resonances. In summary, the ^{31}P (and ^6Li) results strongly imply that both the LiFePO_4 and FePO_4 clusters are larger than

just one coordination shell, so that significant concentrations of intermediate environments do not exist.

All the resonances observed in the different spectra could be correlated with the presence of a particular phase detected by XRD, except in the case of the extremely weak impurity peak seen for SC0.14 (and the corresponding batch of LiFePO_4 , see above). This correlation again indicates that no noticeable amounts of amorphous phases containing lithium and/or phosphorus, that could not be detected by diffraction, exist in the samples, consistent with previous TEM results.¹⁵

Variable temperature NMR. ^7Li MAS NMR spectra obtained at a series of different temperatures for the different samples are shown in Figure 6. Deconvolution of the isotropic peaks was performed, and the resulting peak shifts and widths are plotted against $1/T$ in Figure 7. The larger hyperfine and dipolar couplings associated with ^7Li relative to ^6Li ,⁵² combined with the less efficient averaging of these interactions due to the use of a slower spinning speed in these experiments, produce spectra with lower resolution than those shown in Figure 3. As a consequence, the spectrum of SC0.74 could be fit with just one resonance, as opposed to the two needed to account for the lineshape observed in the high-speed ^6Li spectrum. The position of this resonance (-38 ppm) appears at a position that corresponds to the weighted average of the two resonances used to fit the ^6Li spectrum. In the case of SC0.14, although two peaks could be resolved at room temperature, only one peak with much larger width was sufficient to fit the data at higher temperatures, an indication that the original resonances shift toward each other and either become less resolved, or even merge, upon heating. For

comparison, the result obtained by fitting the room temperature spectrum of SC0.14 with a single broad resonance (located at approximately -36 ppm) is also shown in Figure 7a. The center of gravity of the spectrum is seen to move toward higher frequencies from room to higher temperature, the -36 ppm resonance following this trend. The location of this averaged resonance appears at a lower frequency (i.e., with a more negative shift) than that of $\text{Li}_{0.6}\text{FePO}_4$ in the SC0.54 sample and closer to the shift from SC0.74 ($33\%\text{LiFePO}_4 + 67\%\text{Li}_{0.6}\text{FePO}_4$), implying that the environments probed by the lithium ions in $\text{Li}_{0.34}\text{FePO}_4$ contain more Fe^{2+} than the Li local environments in $\text{Li}_{0.6}\text{FePO}_4$. Again, this is consistent with large LiFePO_4 -like clusters in $\text{Li}_{0.34}\text{FePO}_4$ (in SC0.14).

A general tendency for a decrease in both the width of the peaks and the absolute value of the shift with increasing temperature is observed for SC0.14, SC0.54 and SC0.74. Strikingly, the trend does not seem to be continuous, a noticeable change in slope in the plots for both shift and linewidth being seen in all cases above 125°C ($1/T=0.0025 \text{ K}^{-1}$). In general, a peak shift toward lower absolute values, accompanied by narrowing, is expected in paramagnetic samples due to the corresponding decrease in the magnetic susceptibility of the transition metal ions. However, this dependence should be close to linear and have a constant slope in the absence of a magnetic or structural phase transition. Antiferromagnetic transitions have been reported for LiFePO_4 and FePO_4 at 50K and 125K, respectively, and Curie-Weiss behavior has been reported at the temperatures studied here.^{40, 53} Thus, the discontinuity should reflect a noticeable change in electronic structure (as probed by Li), consistent with formation of the solid solution phases^{7, 10} and/or (additional) mobility between 150°C and 200°C . This point is discussed in more detail below.

The nature of the transition is very different for the SC0.54/SC0.74 and NHT0.62 samples. As NHT0.62 (a previously unheated mixture of LiFePO_4 and FePO_4) is heated, discontinuous behavior is observed. At 100°C , a weak resonance at approximately -10 ppm is observed (Figure 6) whose intensity grows steadily as the temperature is increased, at the expense of the original one (Fig. 7c). This new peak is ascribed to $\text{Li}_{0.6}\text{FePO}_4$ and dominates the spectrum at 250°C , only a small, lower frequency shoulder remaining (Fig. 7c). Within error, the shift of the Li signal of the $\text{Li}_{0.6}\text{FePO}_4$ phase mirrors that of the SC0.54 sample, consistent with this assignment. Similar mixtures have been shown by XRD to initially form $\text{Li}_{0.6}\text{FePO}_4$ before converting into single-phase solid solutions,¹⁰ but the process, as probed by NMR, appears to have started at a lower temperature ($75\text{-}100^\circ\text{C}$) than in the XRD experiments ($150\text{-}200^\circ\text{C}$).^{7, 10} This is ascribed to the ability of NMR to detect smaller particles (i.e., with crystalline domains that are smaller than the coherence length probed by XRD). Previous TEM results revealed that the precipitated phases (or phase segregated domains) in cooled crystals are distributed along the b direction with ac phase boundaries, whereas in large micron-sized unheated crystals formed by chemical delithiation, the end member phases are located in stripes that alternate along the a direction with phase boundaries in the bc plane.¹⁵ Since the lithium mobility is much greater in the b direction than in either the a or c direction⁵⁴ it is reasonable to expect that kinetically it will be much easier to achieve a uniform Li distribution in the preheated crystals, where the different phases exist within one crystallite. Thus, the behavior of the NHT sample is ascribed to gradual mixing of the LiFePO_4 and FePO_4 phases (involving Li migration between particles) to slowly form the $\text{Li}_{0.6}\text{FePO}_4$ phase (which gives rise to the -10 ppm resonance at 100°C), the

concentration of this phase increasing with time and temperature. Complete mixing to a single solid-solution phase does not take place in the sample at the temperatures measured here.

SC0.54 shows the highest shift (-1 ppm) at 250°C, followed by SC0.14 (-8.5 ppm) and SC0.74 (-15.5 ppm). If the transformation of the samples from two-phase mixtures to a single-phase solid solution were complete at this temperature, the composition of the final products should be $\text{Li}_{0.14}\text{FePO}_4$, $\text{Li}_{0.54}\text{FePO}_4$ and $\text{Li}_{0.74}\text{FePO}_4$, with increasing $\text{Fe}^{2+}/\text{Fe}^{3+}$ ratios as the lithium content increases. Assuming rapid electronic hopping and/or no or some, but uncorrelated lithium motion, the lithium ions will see a mixed $\text{Fe}^{3+}/\text{Fe}^{2+}$ state, with those in $\text{Li}_{0.14}\text{FePO}_4$ seeing the largest amount of Fe^{3+} . Since this larger amount of Fe^{3+} induces more positive NMR shifts, $\text{Li}_{0.14}\text{FePO}_4$ should show the highest shift, whereas the lowest would correspond to $\text{Li}_{0.74}\text{FePO}_4$, which is clearly not the case. Instead, $\text{Li}_{0.14}\text{FePO}_4$ shows the largest change of the shift vs. $1/T$ (reflected in the largest slope), and it is clear that on extrapolation to higher temperatures, $\text{Li}_{0.14}\text{FePO}_4$ would eventually have the highest shift. This behavior is ascribed to the incomplete formation of a solid solution for $y=0.14$ at the highest temperatures studied in this work.⁹

The ease of formation of solid solutions from mixtures of LiFePO_4 and FePO_4 varies with composition and is known to be sluggish in the temperature range studied here; longer equilibration times or temperatures above 300°C have been shown to be required to prepare samples that show single-phase X-ray diffractograms.⁷⁻⁹ Further, some residual amounts of LiFePO_4 or FePO_4 have been found in the Mössbauer spectra (a technique with a sensitivity to minority phases comparable to that of NMR in this system) of mixtures with different proportions of LiFePO_4 and FePO_4 heated as high as 400°C.¹¹

The transition to solid solution is more facile in samples with compositions closer to the eutectic point in the phase diagram, which is close to $\text{Li}_{0.6}\text{FePO}_4$, and is reported to occur at the highest temperature precisely for mixtures with lithium contents similar to SC0.14.^{7,9}

A noticeable increase in the intensity in the 4000-5000 ppm region is observed in the ^{31}P MAS NMR spectrum when SC0.54 is heated to 250°C (Figure 5). Resolution of isotropic resonances is complicated by the large width of the signals; experiments at different spinning speeds led to the tentative assignment of isotropic peaks at 5775 and 2885 ppm and no distinct ones could be identified around 4000-5000 ppm. Nonetheless, phosphorus environment(s) with mixtures of Fe^{3+} and Fe^{2+} , which appear to be related to the existence of the resonance at 4930 ppm seen at room temperature in the fast MAS spectrum (Figure 4), are clearly present. Interestingly, the linewidths of the peaks from 2000 to 5000 ppm (i.e., corresponding to all Fe^{2+} and mixed $\text{Fe}^{3+}/\text{Fe}^{2+}$ environments) increase noticeably, while that of the 5930 ppm (all- Fe^{3+}) is similar, again suggesting that it partially arises from a separate phase (i.e., FePO_4). The increase in linewidth indicates that a motional and/or chemical process is entering the timescale probed by the ^{31}P MAS NMR experiment.

Finally, the isotropic resonances in the ^7Li MAS NMR spectra of the samples cooled to room temperature after the heat treatment in the NMR setup are compared to those recorded before the experiment was performed (Fig. 8). A displacement of the center of gravity toward less negative values can readily be observed for NHT0.62, in accordance with the precipitation of the intermediate $\text{Li}_{0.6}\text{FePO}_4$ phase on cooling, and in agreement with previous XRD results.¹⁰ In contrast, spectra of the other three samples

were almost identical at room temperature before and after the NMR heating studies, indicating that, once the samples have been heat-treated, successive treatments produce changes that are largely reversible.

Discussion

Electron-lithium mobility in Li_xFePO_4 . The MAS NMR results in this paper offer insight in the structural order in the different Li_xFePO_4 phases present in the samples studied, but should also provide information regarding the mobility of electrons and lithium ions through their crystal lattice. Recent studies by two groups have used ^{57}Fe Mössbauer spectroscopy (MS) data at different temperatures to determine the existence and extent of charge-carrier motion in the $\text{Li}_{0.6}\text{FePO}_4$ intermediate phase.^{11, 13, 14} Well-resolved Fe^{2+} and Fe^{3+} doublets were observed in the room temperature spectra. These doublets broaden and eventually coalesce into a single one at elevated temperatures, the exact temperature of coalescence varying between samples. The presence of only one signal is indicative of the existence of, at a minimum, electron hopping between the iron ions. Further, linear fits of the spectral parameters vs. $1/T$ to an Arrhenius-type function led to measurements of the activation energy, E_a , and the pre-exponential factor (attempt frequency), ν , defining the kinetics of the motional processes. However, the analysis and range of temperature employed differs between the two groups and between different papers, as did the samples and their thermal processing, and, therefore, a range of values was reported for these parameters. Ellis *et al.* use the data above 250 °C for a sample initially composed of 55% LiFePO_4 +45% FePO_4 to fit the (corrected) line width variation of the signal assigned to the solid solution $\text{Li}_{0.55}\text{FePO}_4$, which results in an activation

energy, E_a , of 775 ± 108 meV.¹¹ The fact that this activation energy is much larger than that predicted for free polaron mobility, as obtained by first principles calculations,⁵⁵ was ascribed to the existence of concerted lithium and electron hopping at these temperatures. Dodd *et al.*¹³ and Tan *et al.*¹⁴ investigated single-phase quenched $\text{Li}_{0.6}\text{FePO}_4$ samples (i.e., samples that are similar to our Q0.54), and found that the MS Fe^{2+} and Fe^{3+} signals start to shift toward each other above 130-150°C and have almost coalesced at 240°C, which, again, was taken as an indication of the presence of electron hopping. Values of both E_a and ν were obtained by fitting both the isomer shifts and quadrupole splittings (instead of the peak width) vs. $1/T$ plots above 130°C. The former were used to analyze the kinetics of the electron hopping, and a range of values was calculated. Dodd *et al.*¹³ report $E_a = 700 \pm 100$ meV, $\nu = 6 \cdot 10^{14}$ Hz for Fe^{2+} and $E_a = 500 \pm 100$ meV, $\nu = 1 \cdot 10^{13}$ Hz for Fe^{3+} , while Tan *et al.*,¹⁴ in a later paper from the same group, report $E_a = 560$ meV, $\nu = 2 \cdot 10^{13}$ Hz for both Fe^{2+} and Fe^{3+} . The discrepancy in values, even between Fe^{2+} and Fe^{3+} in a process that necessarily involves both, is considered to be within error, according to the authors. Interestingly, the onset for the progressive reduction of the quadrupole splitting of the Fe^{2+} signals is observed at a lower temperature of around 100°C, in both reports. Indeed, fitting the data leads to $E_a = 335 \pm 25$ meV, $\nu = 5 \cdot 10^{11}$ Hz (according to Dodd *et al.*)¹³ and $E_a = 511$ meV, $\nu = 2 \cdot 10^{13}$ Hz (according to Tan *et al.*)¹⁴ for this dynamic alteration of the electric field gradient (EFG) around Fe^{2+} . The authors hypothesize that the differences in onset temperature and E_a , as calculated from the isomer shift and the quadrupolar splitting, arise from the existence of lithium motion that is decoupled from electron mobility. Since Li^+ is more often in the vicinity of Fe^{2+} , it is expected that the Fe^{2+} ions will be more affected by the Li^+ mobility, hence the larger

variability observed in the values for this ion. This hypothesis suggests that, while lithium-electron motion may be correlated above 150°C, some uncoupled lithium motion may exist at lower temperatures.

The resolution of different isomer shifts for Fe²⁺ and Fe³⁺ in the Mössbauer spectra of Li_{0.6}FePO₄ does not necessarily imply that electron motion does not occur. For signal averaging to occur, motion must be faster than the frequency separation of the two signals, which is about 11.5 MHz ($\Delta E = \frac{\Delta\delta_{IS} \cdot E_{\gamma}}{c}$, where $\Delta\delta_{IS}$ - equal to the separation between the Fe²⁺ and Fe³⁺ isomer shifts- ≈ 1 mm/s^{13, 14}, c is the speed of light in vacuum and E_{γ} is the Mössbauer gamma energy). In stark contrast, NMR is typically sensitive to process occurring at timescales in the tens or hundreds of Hz, which makes it a probe of slower motional processes. The available MS data will be used here in order to evaluate whether the single resonance observed in the ⁶Li MAS NMR data of SC0.54 (or Q0.54, Fig. 3) could be due to the existence of the electron and/or lithium hopping processes in the Li_{0.6}FePO₄ phase that are observed by MS above 100-150°C. To this end, the hop-rates were extrapolated to room temperature using the Arrhenius equation. Given the variability of E_a and ν values found in the literature, those that lead to the largest and smallest hop frequencies were used. The highest possible hopping rate at room temperature, $3.5 \cdot 10^4$ Hz was obtained by using the data for Fe³⁺ given by Dodd *et al.* ($E_a=500$ meV, $\nu=1 \cdot 10^{13}$ Hz)¹³ and can, hence, be considered as an upper limit for hopping. Likewise, the lower limit for hopping, obtained by using the Fe²⁺ data ($E_a=700$ meV, $\nu=6 \cdot 10^{14}$ Hz) by the same authors, corresponds to 870 Hz. Coalescence between two resonances in a 1-dimensional NMR spectrum occurs when the frequency for

exchange between the two sites occurs with a frequency that is greater or equal to $\frac{1}{2}\pi\nu_{AB}$, where ν_{AB} is the frequency separation between the two resonances, A and B.⁵⁶

Thus, the range of hop rates above will result in coalescence if the ^6Li peak separations

are less than *ca.* 540 ($\delta = \frac{3.5 \cdot 10^4 \text{ Hz}}{2^{-1/2} \cdot \pi} \cdot 10^6 \text{ ppm} \approx 540 \text{ ppm}$; upper limit) and 14 ppm

(lower limit). Higher rates are required for coalescence of the ^7Li resonances, since the separations are larger in units of Hz, and only resonances with separations lower than 200 and 5 ppm would be affected by these hop rates. [These estimates lie within the range of

hyperfine shifts observed for lithium environments in LiFePO_4 that contain Fe^{2+} and Fe^{3+} ,⁴³ and in principle, are consistent with the existence of hopping at room temperature

and the subsequent observation of a single resonance for $\text{Li}_{10,6}\text{FePO}_4$. The value calculated based on the lower limit may not be sufficient for averaging, but at the very least, if coalescence does not occur at room temperature, even small increases in

temperature, which will result in both a decrease in separation between the resonances due to the change in magnetic susceptibility of the sample and an increase in hop

frequency, would be sufficient to induce averaging. A similar behavior has already been reported for LiMn_2O_4 , which contains both Mn^{3+} and Mn^{4+} , the rapid electronic (small

polaron) hopping resulting in a single local environment for Li.¹⁷ [Interestingly, while hopping would seem to be fast to allow the different ^6Li resonances to be resolved, at

least just above room temperatures, it would clearly still be too slow to average the ^{31}P

NMR signals. Even using the highest value of $3.5 \cdot 10^4$ Hz, the maximum peak separation

that would be averaged by motion would be *ca.* 194 ppm ($\partial = \frac{3.5 \cdot 10^4 \text{ Hz}}{2^{-1/2} \cdot \pi} \cdot 10^6 \text{ ppm}$),

clearly much smaller than that observed here (*ca.* 3000 ppm, Figure 4).

While the hop frequency calculations appear consistent with signal averaging due to electron hopping at close to room temperature, a couple of factors cast a reasonable doubt onto this hypothesis. First, the large variations in the reported activation energies introduce considerable uncertainty into the extrapolations. The second factor has to do with the discontinuity in the shift and peak width vs. $1/T$ plots of SC0.54 and SC0.74 above 125°C (Figs. 7a, b), discussed in the previous section. This discontinuity occurs below the reported eutectic temperature in the $\text{LiFePO}_4\text{-FePO}_4$ phase diagrams available in the literature (200 °C).^{7,9} In our samples, the kinetics associated with mixing are likely to be easier as they occur in the same particles, which, together with the higher sensitivity of NMR to small amounts of a particular phase than diffraction, may make our measurements closer to the true eutectic temperature. The phase mixing that will occur above this temperature on the phase diagram, will necessarily affect the NMR signals, but it may not be the sole cause of this discontinuity. Taking SC0.54 as an example, which contains 10% FePO_4 and 90% $\text{Li}_{0.6}\text{FePO}_4$ (Table 1), it is expected that the lithium content of the $\text{Li}_{0.6}\text{FePO}_4$ phase will decrease gradually, to approach the overall composition, $\text{Li}_{0.54}\text{FePO}_4$ as the temperature is increased. At the same time, there will be an increase in solubility of Li within FePO_4 , concomitant with a decrease in the concentration of this phase; such a change should generate a novel ^7Li NMR resonance with an even more positive frequency. Both factors will result in an increase in slope of the ^7Li signal, due to the larger number, on average, of Fe^{3+} ions, which have a larger magnetic

susceptibility, nearby Li^+ . In turn, when SC0.74 is heated above the eutectic temperature, the Li content of this phase should *increase*, so the slope should become smaller. At the same time, the Li content of the LiFePO_4 component should decrease, resulting in a more positive shift and a larger slope. When this process starts to occur, the overall change will reflect the balance between the variations in limits of solubility of the two components. Clearly, the compositions in SC0.74 and SC0.54 above the eutectoid point should be different, yet the slopes, which are dependent on the $\text{Fe}^{3+}/\text{Fe}^{2+}$ ratio nearby Li in the phases, above 125°C are similar, within error, for both compounds. Since both samples initially contain $\text{Li}_{0.6}\text{FePO}_4$, it is likely that the transition could be associated with other phenomena apart from simply phase mixing, including the onset or a change in the nature of the electronic mobility. This conclusion implies that definitively determining whether such motion already occurs at room temperature and, hence, is responsible for the observation of a single Li resonance for $\text{Li}_{0.6}\text{FePO}_4$ is not possible, at this point. However, the increase in slope above 125°C does appear to suggest that the average Fe oxidation state probed by a lithium ion increases gradually, resulting in a shift to higher frequency that is greater than that based on extrapolating the low temperature data. Such increase implies that, at room temperature, Li^+ is on average closer to more Fe^{2+} ions than expected based on a random distribution of Li^+ and electron holes, i.e., that there is some correlation between these two, at lower temperatures: Motion involving both a lithium ion and an electron will not affect the hyperfine shift of the lithium environment, but only uncorrelated hops of electrons between Fe^{3+} and Fe^{2+} ions or of Li^+ into sites nearby more Fe^{3+} . The NMR data above 125°C clearly suggests a steady increase with temperature of the rate of uncorrelated electron hopping. The high

temperature (250 °C) ^{31}P data of the SC0.54 suggests that the motional processes in $\text{Li}_{0.6}\text{FePO}_4$ are more complex than suggested by a simple two-site exchange process involving the Fe^{2+} and Fe^{3+} spins. Based on the available MS data,^{13, 14} extremely rapid exchange should be occurring in the MHz timescale, independent of which model is used to calculate the mobility. In contrast, although our ^{31}P data do show evidence for mobility involving electron hopping (increased ^{31}P lineshapes), the motion has not resulted in a single ^{31}P resonance (and thus motion *involving all the sample* cannot be in the MHz timescale). Two important points can be made, however, (1) the shift of the 3020 ppm to only 2885 ppm is much smaller than expected based on a $1/T$ dependence of temperature.⁴⁶ This indicates that the ^{31}P environments that give rise to this environment are on average nearby more Fe^{3+} ions than at lower temperature. This is consistent with rapid electron mobility, on a timescale that is faster than the NMR timescale, consistent with both the MS and ^7Li NMR results. (2) The lack of total signal averaging must indicate that either the samples are inhomogeneous and/or that the signal averaging affects different local environments differently. Both explanations are consistent with some MS data, particularly at lower temperatures, where evidence for the distributions in the timescale of hopping are often seen (e.g., residual signals due to Fe^{3+} and Fe^{2+} components).

In the case of the $\text{Li}_{0.34}\text{FePO}_4$ fraction found in SC0.14, at least two distinct resonances could be resolved by ^6Li MAS NMR at -1 and -63 ppm (Fig. 3). The electron frequency hopping rates were again calculated using the MS data reported for a similar solid solution phase ($\text{Li}_{0.3}\text{FePO}_4$),¹⁴ using the two different E_a values provided for Fe^{2+} (543 meV) and Fe^{3+} (572 meV), with ν fixed to $2 \cdot 10^{13}$ Hz. These values result in

hopping frequencies at room temperature of more than $1.3 \cdot 10^4$ and $4.2 \cdot 10^3$ Hz, respectively, which, in turn, will result in coalescence for resonances separated by less than 66-203 ppm (24-76 ppm for ^7Li). These values are very close to the peak separation seen in this system (62 ppm), and thus, assuming the hopping scenario applies at this temperature, some signal averaging or, at a minimum, peak broadening, is expected, for a simple motion that results in an averaging of the Li environments that give rise to these sites. In this phase, however, at least two resonances were observed by NMR, indicating that complete averaging does not occur in this phase. Nonetheless, at this point, the existence of motional schemes involving motion between a subset of lithium sites that would lead to a situation in which the peak at -1 ppm would itself be the result of such partial averaging cannot be excluded.

Only a slight increase in temperature is enough to reduce the resolution of the SC0.14 spectra, and by only 75-100°C, a single, albeit broad, signal is seen (Fig. 6). These observations suggest that mobility around temperature, if existent, is sluggish, but that heating does result in some motion that is now on the NMR timeframe. The fact that the averaged resonance still has a shift that corresponds to the center of gravity of the resonances seen at lower temperatures, suggests that any motion at this point involves correlated lithium-electron mobility, so that the new averaged environments do not contain more Fe^{3+} than those when no motion takes place, an indication that the $\text{Li}^+ - \text{Fe}^{2+}$ interaction remains strong. In contrast, as in the case of SC0.54 and SC0.74, a change in the rate of shift increase is observed above 125°C, which is ascribed to an increase in Fe^{3+} in the average Li environment and, thus, to the onset of some uncorrelated electron (and possibly lithium) motion at these temperatures, as proposed for $\text{Li}_{0.6}\text{FePO}_4$. To result in

mixing of the phases, Li mobility within the tunnels must occur, but this process does not have to be rapid.

Further insight into the mobility within $\text{Li}_{0.6}\text{FePO}_4$ and $\text{Li}_{0.34}\text{FePO}_4$ can yet be obtained from more detailed analysis of the variable temperature ^7Li NMR data. As noted above, the averaged Li environment in $\text{Li}_{0.6}\text{FePO}_4$ (whether taken at room temperature or at 125°C) systematically resonates at higher frequencies than that of $\text{Li}_{0.34}\text{FePO}_4$ within the temperature range observed here (see SC0.54 and SC0.14 in Fig. 7a), an indication of the existence of lithium ions in environments that are richer in Fe^{3+} in the former. Such observation must mean that the lithium environments in $\text{Li}_{0.6}\text{FePO}_4$ are nearby more Fe^{3+} ions than in $\text{Li}_{0.34}\text{FePO}_4$. In other words, the $\text{Li}^+-\text{Fe}^{2+}$ interaction, i.e., the Li^+-e^- correlation (which would slow –or even prevent– polaron hopping and favor $\text{Li}^+-\text{Fe}^{2+}$ clustering), in $\text{Li}_{0.6}\text{FePO}_4$ is weaker than in $\text{Li}_{0.34}\text{FePO}_4$. Such conclusion is in apparent contradiction with the higher binding energies predicted for the vacancy-hole interaction in $\text{Li}_{1-x}\text{FePO}_4$ ($x=1/64$) compared to the lithium-electron interaction in Li_yFePO_4 ($y=1/64$), as predicted by GGA+U calculations.⁵⁵ However, these calculations were performed for very low Li^+ vacancy/hole concentrations, so a comparison with our samples may not be appropriate. It is likely that, as the vacancy (hole) concentrations increase to close to 0.5, the number of vacancy-vacancy (hole-hole) interactions increase, along with the screening (i.e., the polarons are less effectively localized), resulting in a reduction in the apparent strength of the $\text{Li}^+-\text{Fe}^{2+}$ ordering energy.

The difference in Li^+-e^- correlation observed here has implications in terms of both the stability of and ion mobility within these phases. If lithium is strongly correlated with Fe^{2+} in $\text{Li}_{0.34}\text{FePO}_4$, the tendency to form domains with marked charge differences

would eventually lead to the disproportionation to LiFePO_4 and FePO_4 . Indeed, it could be argued that, at short length scales, this process has already occurred. Such driving force toward disproportionation may be at the origin the low stability of this phase, which demixes more rapidly than $\text{Li}_{0.6}\text{FePO}_4$. Computational studies in which a strong $\text{Li}^+ - e^-$ correlation was predicted to be at the origin of the low stability of Li_xFePO_4 solid solutions⁵⁷ are in agreement with this decomposition mechanism. Conversely, the weaker correlation between electrons and lithium ions in $\text{Li}_{0.6}\text{FePO}_4$ may allow the creation of Fe^{3+} -richer lithium environments that could contribute to its higher stability through an increase in entropy.

Finally, three additional points are worth noting. First, the stability of different compositions within the same particles will strongly depend on the interfacial energies between the two phases. Furthermore, the role that these interfacial energies will play in causing demixing of the Li_xFePO_4 will depend on the shapes of the particles.⁵⁸ Demixing along the b -axis of the crystal, as is the case in the samples studied here, causes an interface between two phases in the ac plane. The formation of such interface may be impeded in anisotropic crystals that are extremely thin along the b direction, which, therefore, may not readily demix according to the mechanism proposed in previous work¹⁰ and investigated in this paper. The immediate implication would be that shape may also play a role in controlling the eutetic temperatures in this system, which may account for variations in the eutetic temperatures. Second, although lithium mobility is often discussed in this system, motion can only readily occur along the b -direction, at least for the particle sizes relevant to battery chemistry.^{55, 59, 60} Although such mobility is possible in compositions such as $\text{Li}_{0.6}\text{FePO}_4$ as there are vacancies in the tunnels, it can

only be limited in range, probably only involving hops backwards and forwards between adjacent sites. In contrast, electron mobility can, at least, occur in two dimensions in the bc plane, the FeO_6 octahedra being separated by PO_4 units in the a direction. Mobility in the c direction occurs via zig-zag hops in the $[011]$ direction, involving iron ions that are near Li^+ in different tunnels. Long-range mobility in the c -direction cannot be correlated with a simple Li^+ hop so that the same Li^+ remains nearby the same electron hole throughout. More complex mechanisms are possible where different electron hops require the involvement of different Li^+ in different tunnels, but an, at least, partially uncorrelated motion appears more plausible. Third, although long-range Li hopping will not be significant, particularly for $\text{Li}_{0.6}\text{FePO}_4$, Li mobility may be easier in the case of $\text{Li}_{0.34}\text{FePO}_4$, once uncorrelated motion occurs, since there are more vacancies, and a mechanism whereby the Li in the LiFePO_4 clusters in this phase can gradually “escape” from the Li-rich clusters, as the temperature increases, into the FePO_4 domains, is extremely plausible.

Conclusions

A combination of room and high (up to 250°C) temperature ^6Li , ^7Li and ^{31}P MAS NMR data was used to evaluate the local structure and charge carrier mobility in two metastable solid solution phases in the LiFePO_4 - FePO_4 phase diagram, $\text{Li}_{0.34}\text{FePO}_4$ and $\text{Li}_{0.6}\text{FePO}_4$, which are formed as part of mixtures with FePO_4 or LiFePO_4 by during the decomposition of the corresponding high temperature Li_xFePO_4 solid solution when cooled from 375°C .

$\text{Li}_{0.6}\text{FePO}_4$ is obtained when the overall lithium content is higher than 0.5 (in Li_xFePO_4) and is found to appear as an intermediate when a mixture of 62% LiFePO_4 and 38% FePO_4 are heated. However, the onset of phase nucleation is found to be at lower temperature than previously reported using diffraction data, most likely due to the higher sensitivity to very small domains of NMR. The ^6Li and ^{31}P MAS NMR spectra at room temperature support the existence of a certain degree of local structural order. Mobility within the framework was probed acquiring ^7Li MAS NMR spectra at different temperatures. At this point, we cannot be definitive about the extent of motion at room temperature. Upon heating, a discontinuity in the linear increase in shift above 125°C is observed, which is assigned to a combination of temperature-induced phase mixing between $\text{Li}_{0.6}\text{FePO}_4$ and $\text{LiFePO}_4/\text{FePO}_4$ (depending on the sample) and to the onset of, at least partially, uncorrelated electron- Li^+ motion within the structure. The increase in slope of Li shift vs. inverse temperature after this discontinuity indicates that there is a tendency for Li^+ to order nearby Fe^{2+} in $\text{Li}_{0.6}\text{FePO}_4$ at lower temperature, but that the average Fe oxidation state probed by the Li^+ ions increases gradually above 125°C .

Contrary to $\text{Li}_{0.6}\text{FePO}_4$, the room temperature data of $\text{Li}_{0.34}\text{FePO}_4$ clearly prove the existence of LiFePO_4 -like clusters within the crystal lattice, and suggest that mobility is either very slow or non-existent. Motional processes are activated early on when temperature is raised. A single ^7Li MAS NMR resonance is seen at $75\text{-}100^\circ\text{C}$ which is ascribed to mobility and/or poorer resolution due to the smaller shifts seen at higher temperatures. The new averaged resonance appears at shifts that are at the center of gravity of the resonances at room temperature, indicating that any mobility does not increase the presence of Fe^{3+} in the environments. Such observations are proof that

strong Li^+ - Fe^{2+} interactions exists in this phase. An onset for a new motional process, occurring simultaneous to $\text{Li}_{0.34}\text{FePO}_4/\text{FePO}_4$ mixing in the sample, is again observed above 125°C. Comparison of the shift values obtained at different temperatures for $\text{Li}_{0.6}\text{FePO}_4$ and $\text{Li}_{0.34}\text{FePO}_4$ leads to the conclusion that the Li-Fe^{2+} correlations are stronger in the latter, which may explain the existence of strong LiFePO_4 -clustering.

This paper has outlined a number of scenarios for motion within the structures of the two metastable solid solution phases prepared here. While the limited motion that seems to be taking place below 125°C must involve correlated lithium-electron mobility, our data suggest that at least partially uncorrelated motion does exist when the higher temperatures are used. These scenarios for mobility and, more specifically, the exact nature of the processes above 125°C will be investigated in more detail in future reports.

Acknowledgement. This work was supported by the Assistant Secretary for Energy Efficiency and Renewable Energy, Office of Vehicle Technologies of the U.S. Department of Energy under Contract No. DE-AC02-05CH11231 via subcontract No. 6517749 with the Lawrence Berkeley National Laboratory. JC is indebted to Generalitat de Catalunya for funding through a Beatriu de Pinós fellowship.

Supporting Information Available: ^7Li MAS NMR spectra of pristine LiFePO_4 . This material is available free of charge via the Internet at <http://pubs.acs.org>.

References

1. Tarascon, J. M.; Armand, M., *Nature* **2001**, *414*, 359.

2. Armand, M.; Tarascon, J. M., *Nature* **2008**, *451*, 652.
3. Padhi, A. K.; Nanjundaswamy, K. S.; Goodenough, J. B., *J. Electrochem. Soc.* **1997**, *144*, 1188.
4. Zaghbi, K.; Charest, P.; Guerfi, A.; Shim, J.; Perrier, M.; Striebel, K., *J. Power Sources* **2004**, *134*, 124.
5. Meethong, N.; Huang, H. Y. S.; Speakman, S. A.; Carter, W. C.; Chiang, Y. M., *Adv. Funct. Mater.* **2007**, *17*, 1115.
6. MacNeil, D. D.; Lu, Z. H.; Chen, Z. H.; Dahn, J. R., *J. Power Sources* **2002**, *108*,
8.
7. Delacourt, C.; Poizot, P.; Tarascon, J. M.; Masquelier, C., *Nat. Mater.* **2005**, *4*,
254.
8. Delacourt, C.; Rodriguez-Carvajal, J.; Schmitt, B.; Tarascon, J. M.; Masquelier, C., *Solid State Sci.* **2005**, *7*, 1506.
9. Dodd, J. L.; Yazami, R.; Fultz, B., *Electrochem. Solid State Lett.* **2006**, *9*, A151.
10. Chen, G.; Song, X. Y.; Richardson, T. J., *J. Electrochem. Soc.* **2007**, *154*, A627.
11. Ellis, B.; Perry, L. K.; Ryan, D. H.; Nazar, L. F., *J. Am. Chem. Soc.* **2006**, *128*,
11416.
12. Stevens, R.; Dodd, J. L.; Kresch, M. G.; Yazami, R.; Fultz, B.; Ellis, B.; Nazar, L. F., *J. Phys. Chem. B* **2006**, *110*, 22732.
13. Dodd, J. L.; Halevy, I.; Fultz, B., *J. Phys. Chem. C* **2007**, *111*, 1563.
14. Tan, H. J.; Dodd, J. L.; Fultz, B., *J. Phys. Chem. C* **2009**, *113*, 2526.
15. Chen, G.; Song, X. Y.; Richardson, T. J., *Electrochem. Solid State Lett.* **2006**, *9*,
A295.

16. Grey, C. P.; Dupré, N., *Chem. Rev.* **2004**, *104*, 4493.
17. Lee, Y. J.; Grey, C. P., *J. Am. Chem. Soc.* **1998**, *120*, 12601.
18. Lee, Y. J.; Wang, F.; Mukerjee, S.; McBreen, J.; Grey, C. P., *J. Electrochem. Soc.* **2000**, *147*, 803.
19. Lee, Y. J.; Eng, C.; Grey, G. P., *J. Electrochem. Soc.* **2001**, *148*, A249.
20. Lee, Y. J.; Grey, C. P., *J. Electrochem. Soc.* **2002**, *2*, A103.
21. Lee, Y. J.; Grey, C. P., *J. Phys. Chem. B* **2002**, *106*, 3576.
22. Lee, Y. J.; Grey, C. P., *Chem. Mater.* **2000**, *12*, 3871.
23. Armstrong, A. R.; Dupré, N.; Paterson, A. J.; Grey, C. P.; Bruce, P. G., *Chem. Mater.* **2004**, *16*, 3106.
24. Ménétrier, M.; Saadoune, I.; Levasseur, S.; Delmas, C., *J. Mater. Chem.* **1999**, *9*, 1135.
25. Chazel, C.; Ménétrier, M.; Croguennec, L.; Delmas, C., *Inorg. Chem.* **2006**, *45*, 1184.
26. Marichal, C.; Hirschinger, J.; Granger, P.; Ménétrier, M.; Rougier, A.; Delmas, C., *Inorg. Chem.* **1995**, *34*, 1773.
27. Carlier, D.; Ménétrier, M.; Delmas, C., *J. Mater. Chem.* **2001**, *11*, 594.
28. Yoon, W. S.; Iannopollo, S.; Grey, C. P.; Carlier, D.; Gorman, J.; Reed, J.; Ceder, G., *Electrochem. Solid State Lett.* **2004**, *7*, A167.
29. Yoon, W. S.; Grey, C. P.; Balasubramanian, M.; Yang, X. Q.; Fischer, D. A.; McBreen, J., *Electrochem. Solid State Lett.* **2004**, *7*, A53.
30. Cahill, L. S.; Yin, S. C.; Samoson, A.; Heinmaa, I.; Nazar, L. F.; Goward, G. R., *Chem. Mater.* **2005**, *17*, 6560.

31. Zeng, D.; Cabana, J.; Bréger, J.; Yoon, W. S.; Grey, C. P., *Chem. Mater.* **2007**, *19*, 6277.
32. Bréger, J.; Dupré, N.; Chupas, P. J.; Lee, P. L.; Proffen, T.; Parise, J. B.; Grey, C. P., *J. Am. Chem. Soc.* **2005**, *127*, 7529.
33. Cabana, J.; Dupré, N.; Grey, C. P.; Subias, G.; Caldes, M. T.; Marie, A. M.; Palacín, M. R., *J. Electrochem. Soc.* **2005**, *152*, A2246.
34. Cabana, J.; Dupré, N.; Rousse, G.; Grey, C. P.; Palacín, M. R., *Solid State Ionics* **2005**, *176*, 2205.
35. Wagemaker, M.; Kentgens, A. P. M.; Mulder, F. M., *Nature* **2002**, *418*, 397.
36. Cahill, L. S.; Chapman, R. P.; Britten, J. F.; Goward, G. R., *J. Phys. Chem. B* **2006**, *110*, 7171.
37. Wilkening, M.; Iwaniak, W.; Heine, J.; Epp, V.; Kleinert, A.; Behrens, M.; Nuspl, G.; Bensch, W.; Heitjans, P., *Phys. Chem. Chem. Phys.* **2007**, *9*, 6199.
38. Davis, L. J. M.; Heinmaa, I.; Goward, G. R., *Chem. Mater.* **2009**, *In press*, doi: 10.1021/cm901402u.
39. Chen, G.; Richardson, T. J., *In preparation*.
40. Santoro, R. P.; Newnham, R. E., *Acta Cryst.* **1967**, *22*, 344.
41. Tucker, M. C.; Doeff, M. M.; Richardson, T. J.; Fifiões, R.; Reimer, J. A.; Cairns, E. J., *Electrochem. Solid State Lett.* **2002**, *5*, A95.
42. Tucker, M. C.; Doeff, M. M.; Richardson, T. J.; Fifiões, R.; Cairns, E. J.; Reimer, J. A., *J. Am. Chem. Soc.* **2002**, *124*, 3832.

43. Hamelet, S.; Gibot, P.; Casas-Cabanas, M.; Bonnin, D.; Grey, C. P.; Cabana, J.; Leriche, J.-B.; Rodriguez-Carvajal, J.; Courty, M.; Levasseur, S.; Carlach, P.; Van Thournout, M.; Tarascon, J. M.; Masquelier, C., *J. Mater. Chem.* **2009**, *19*, 3979.
44. Recham, N.; Casas-Cabanas, M.; Cabana, J.; Grey, C. P.; Jumas, J. C.; Dupont, L.; Armand, M.; Tarascon, J. M., *Chem. Mater.* **2008**, *20*, 6798.
45. Kim, J.; Middlemiss, D.; Zhou, B.; Masquelier, C.; Grey, C. P., *In preparation*.
46. Wilcke, S. L.; Lee, Y. J.; Cairns, E. J.; Reimer, J. A., *Appl. Magn. Reson.* **2007**, *32*, 547.
47. Shannon, R. D., *Acta Cryst.* **1976**, *A32*, 751.
48. Zhou, B.; Middlemiss, D.; Cabana, J.; Grey, C. P., *In preparation*.
49. Augustsson, A.; Zhuang, G. V.; Butorin, S. M.; Osorio-Guillen, J. M.; Dong, C. L.; Ahuja, R.; Chang, C. L.; Ross, P. N.; Nordgren, J.; Guo, J. H., *J. Chem. Phys.* **2005**, *123*.
50. Miao, S.; Kocher, M.; Rez, P.; Fultz, B.; Yazami, R.; Ahn, C. C., *J. Phys. Chem. A* **2007**, *111*, 4242.
51. Yoon, W. S.; Chung, K. Y.; McBreen, J.; Zaghbi, K.; Yang, X. Q., *Electrochem. Solid State Lett.* **2006**, *9*, A415.
52. MacKenzie, K. J. D.; Smith, M. E. *Multinuclear Solid-State Nuclear Magnetic Resonance of Inorganic Materials*; Pergamon Materials Series; Elsevier: Amsterdam, 2002.
53. Yamada, A.; Takei, Y.; Koizumi, H.; Sonoyama, N.; Kanno, R., *Appl. Phys. Lett.* **2005**, *87*.

54. Nishimura, S.; Kobayashi, G.; Ohoyama, K.; Kanno, R.; Yashima, M.; Yamada, A., *Nat. Mater.* **2008**, *7*, 707.
55. Maxisch, T.; Zhou, F.; Ceder, G., *Phys. Rev. B* **2006**, *73*.
56. Levitt, M. H. *Spin Dynamics: Basics of Nuclear Magnetic Resonance* John Wiley & Sons, Inc.: New York, 2005.
57. Zhou, F.; Maxisch, T.; Ceder, G., *Phys. Rev. Lett.* **2006**, *97*.
58. Wagemaker, M.; Mulder, F. M.; Van der Ven, A., *Adv. Mater.* **2009**, *21*, 2703.
59. Morgan, D.; Van der Ven, A.; Ceder, G., *Electrochem. Solid State Lett.* **2004**, *7*, A30.
60. Islam, M. S.; Driscoll, D. J.; Fisher, C. A. J.; Slater, P. R., *Chem. Mater.* **2005**, *17*, 5085.
61. Andersson, A. S.; Thomas, J. O., *J. Power Sources* **2001**, *97-98*, 498.

TABLES

Table 1. Phase distribution in initially formulated $x\text{LiFePO}_4 \cdot (1-x)\text{FePO}_4$ mixtures, and the heat treatment used to produce the samples investigated in this study.

x	Label	LiFePO_4	$\text{Li}_{0.6}\text{FePO}_4$	$\text{Li}_{0.54}\text{FePO}_4$	$\text{Li}_{0.34}\text{FePO}_4$	FePO_4
0.14, slow cooled	SC0.14				0.41	0.59
0.54, slow cooled	SC0.54		0.90			0.10
0.54, quenched	Q0.54			1.00		
0.62, unheated	NHT0.62	0.62				0.38
0.74, slow cooled	SC0.74	0.36	0.64			

Table 2. Cationic environment of the Li site in LiFePO_4 .^a

Site	Cationic environment	No. of contacts	Angle
Li (M1)	6 Fe (M2)	2	95.4
		2	97.2
		2	111.0
		2	121.5

Table 3. Bond distances and Fe-O-P angles in LiFePO_4 , $\text{Li}_{0.6}\text{FePO}_4$ and FePO_4 (see Figure 2b for labeling).

		LiFePO_4^{61}		$\text{Li}_{0.6}\text{FePO}_4^8$		FePO_4^{61}	
Fe	No. of contacts	Fe-O (Å)	Fe-O-P (°)	Fe-O (Å)	Fe-O-P (°)	Fe-O (Å)	Fe-O-P (°)
a	2	2.25	94.8	2.21	96.0	2.14	96.5
b	2	2.06	128.9	2.05	126.5	2.04	123.8
c	1	2.20	120.3	2.09	125.7	1.94	136.8
d	1	2.11	126.7	2.05	129.9	1.88	136.4

FIGURE CAPTIONS

Figure 1: a) XRD patterns (Cu K α radiation, $\lambda=1.5406$ Å) of LiFePO₄, FePO₄ and the SC0.14, SC0.54 and SC0.74 samples, and zoom-in of the 29.0-31.5° region (inset), b) Comparison of the XRD patterns of SC0.54 and Q0.54, both as prepared and after storage for 5 months.

Figure 2: Coordination around a) Li and b) P in LiFePO₄. The diamond-patterned and crossed dark grey balls depict the central Li and P, respectively. The light grey balls correspond to O and the black balls represent Fe. Selected bond distances and angles are indicated. The letters and numbers in b) indicate symmetrically equivalent O and Fe ions (see table 3).

Figure 3: Spectral deconvolution (green, peaks and red, sum) of the ⁶Li MAS NMR spectra (blue) of the different samples studied in the course of this work, acquired at 38 kHz. Significant shift values are indicated. See table 1 for sample labeling and composition.

Figure 4: ³¹P MAS NMR spectra of LiFePO₄, FePO₄ and the SC0.14 and SC0.54 samples, acquired at 38 kHz. Significant shift values are indicated, whereas the rest of the peaks are spinning sidebands.

Figure 5: ³¹P MAS NMR spectra of SC0.54 and Q0.54, at room temperature, acquired at 20 kHz. The ³¹P MAS NMR spectrum of SC0.54 acquired at 250°C is also shown.

Significant shift values are indicated, whereas the rest of the peaks are spinning sidebands. The dashed rectangle indicates a region where an isotropic resonance is also found; the width of the individual peaks hinders its unequivocal assignment.

Figure 6: Variable-temperature ^7Li MAS NMR spectra of SC0.14, SC0.54, NHT0.62 and SC0.74, acquired at 20 kHz. The temperature values corresponding to each spectrum are indicated; “RT” corresponds to room temperature. The spinning sidebands of the main isotropic peak are marked with asterisks in the highest temperature spectrum. The crosses indicate sidebands produced by an impurity with a shift at around 220 ppm (see text).

Figure 7: a) ^7Li MAS NMR shifts and b) peak full widths at half maximum (FWHM) vs. $1/T$ for SC0.14, SC0.54 and SC0.74, and c) ^7Li MAS NMR shifts and % of intensity of the Li_xFePO_4 intermediate phase vs. $1/T$ for NHT0.62. The data were obtained by deconvolution of the spectra in Figure 5. Note that for SC0.14, the results of the fitting with one (broken line) and two (solid line) peaks of the spectrum at low temperature are provided. The contribution to the isotropic peak from the sideband of the 200 ppm impurity peak is not plotted. In addition, the two peaks related to Li_xFePO_4 phases show very similar widths, so only one point is provided. The estimated shift errors are ± 2 and ± 6 ppm when one and two peaks are present, respectively. FWHM errors are ± 80 Hz and ± 200 Hz when one and two peaks are present, respectively.

Figure 8: Isotropic ^7Li MAS NMR peaks of a) SC0.14, b) SC0.54, c) NHT0.62, d) SC0.74, acquired at room temperature (20 kHz) before and after the variable temperature experiments. The shifts of the peak maxima are marked.

Figure 1.

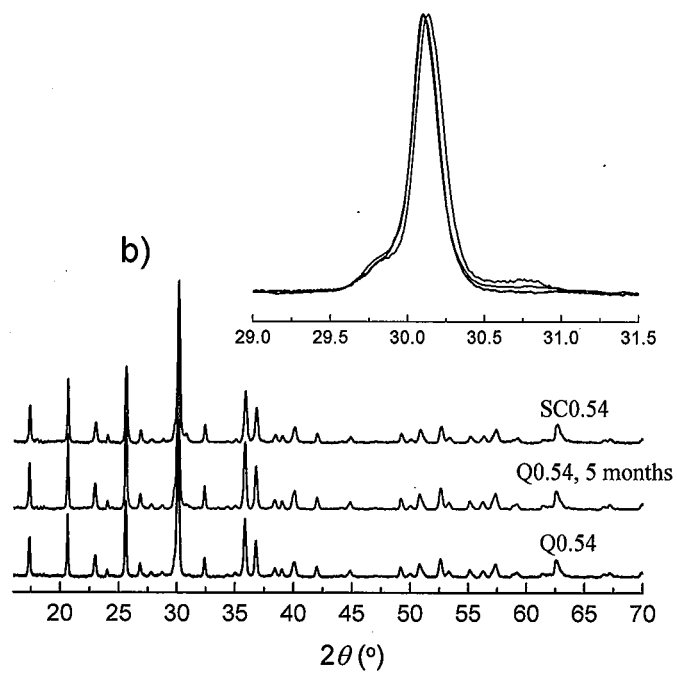
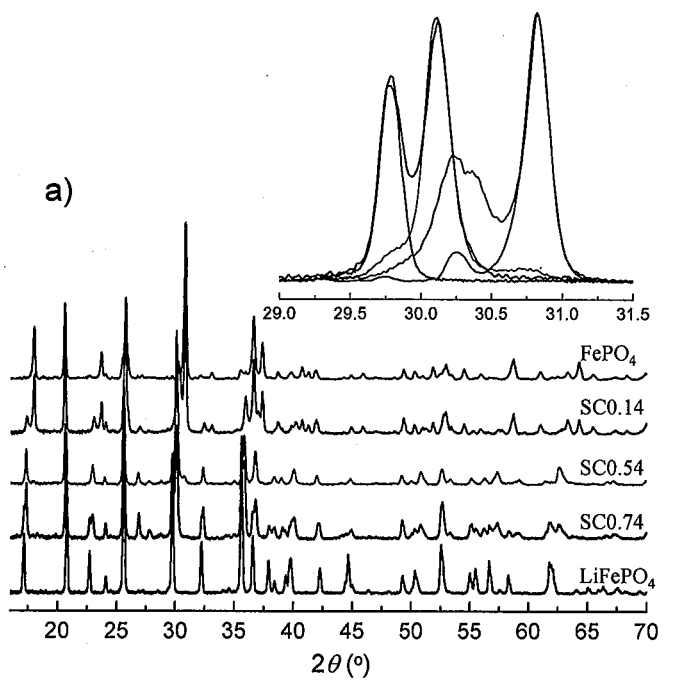


Figure 2.

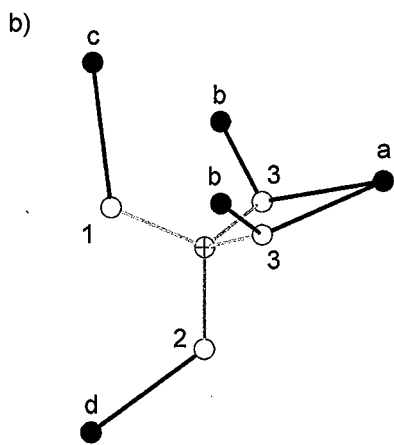
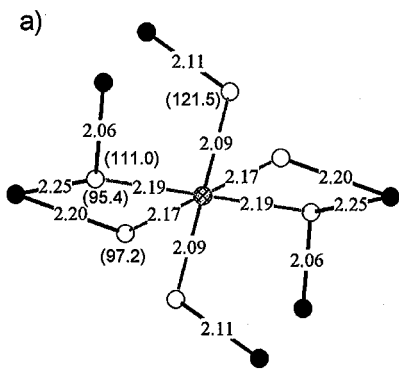


Figure 3.

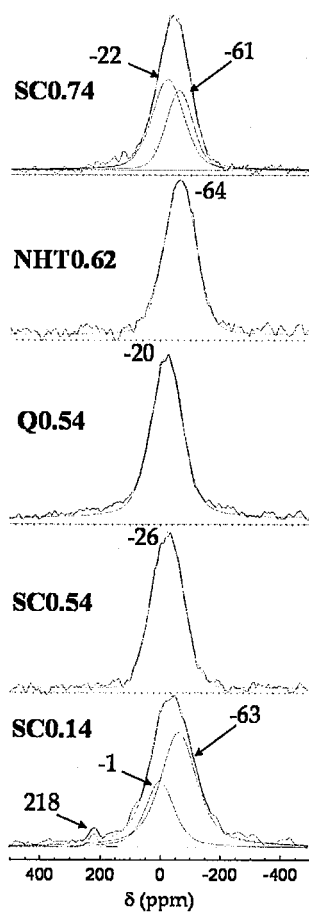


Figure 4.

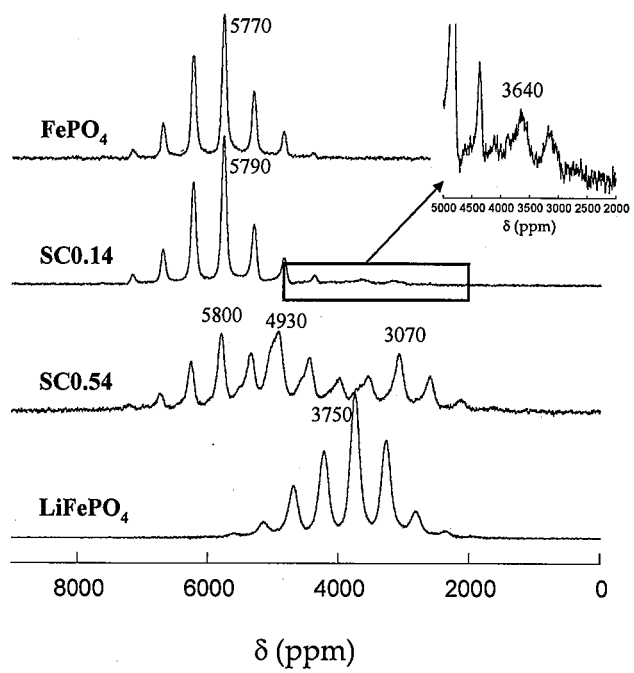


Figure 5.

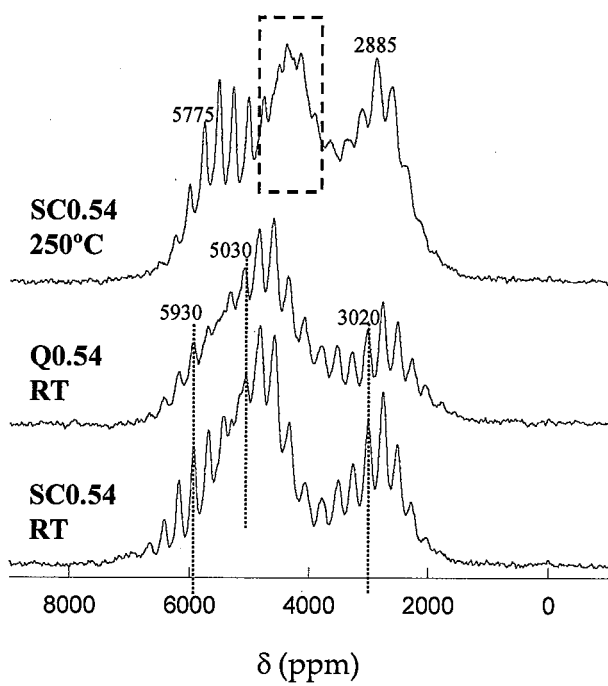
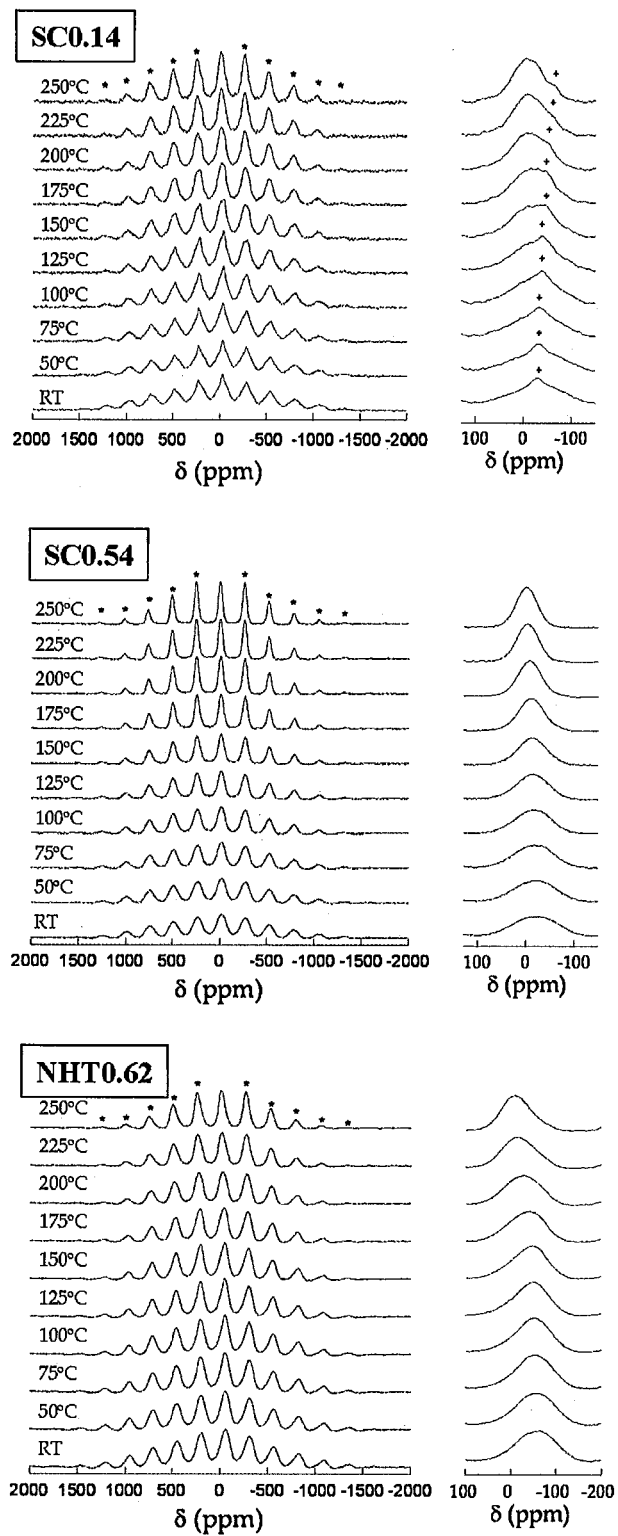


Figure 6.



SC0.74

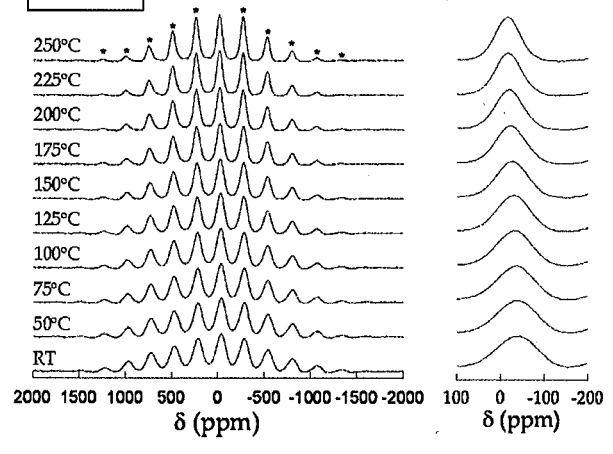


Figure 7.

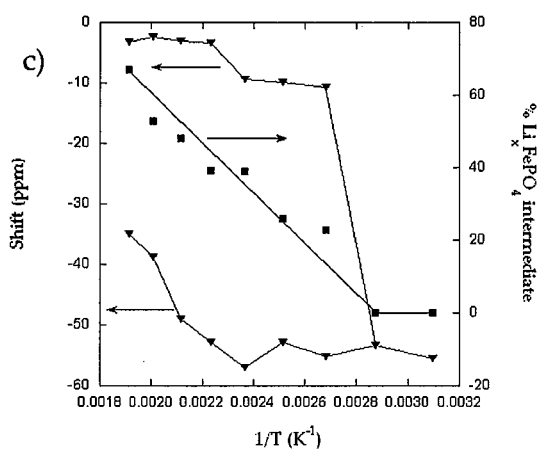
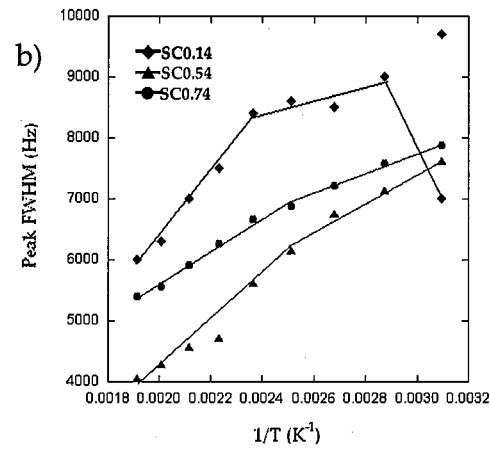
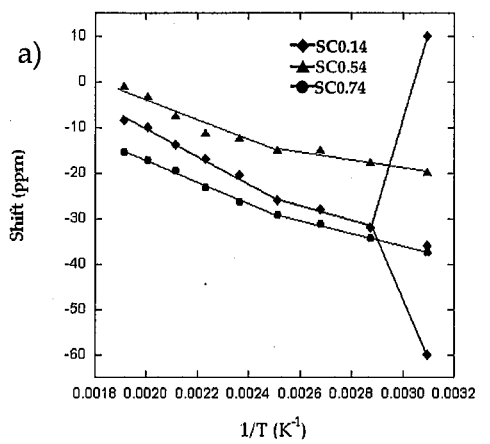
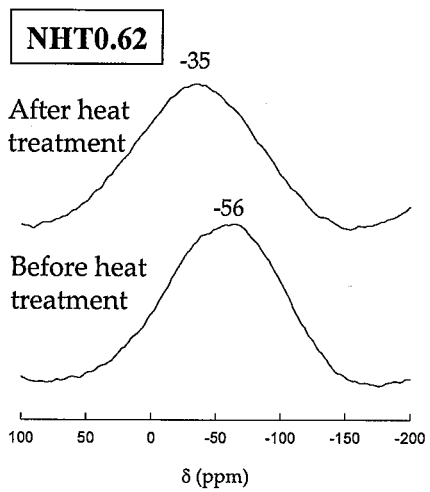
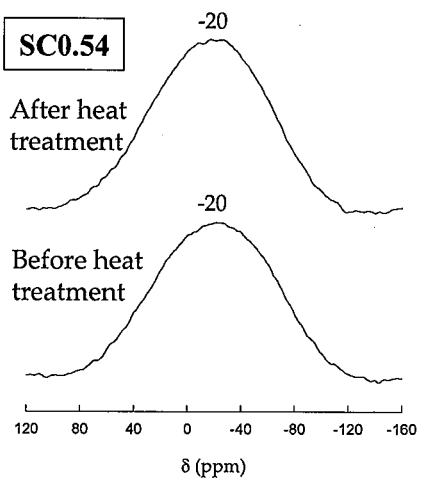
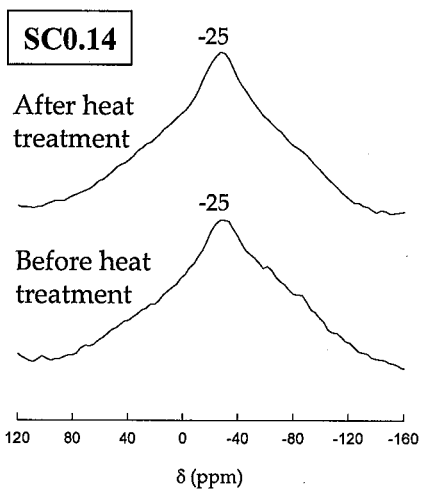


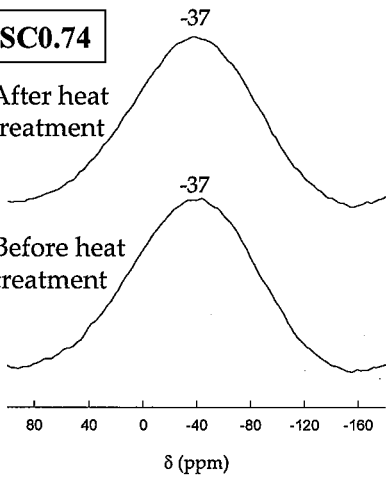
Figure 8.



SC0.74

After heat
treatment

Before heat
treatment



Synopsis TOC

MAS NMR experiments were conducted on a series of samples in the $\text{LiFePO}_4\text{-FePO}_4$ system, containing the end-members and/or two metastable solid solution phases, $\text{Li}_{0.6}\text{FePO}_4$ or $\text{Li}_{0.34}\text{FePO}_4$. Evidence for $\text{Li}^+\text{-Fe}^{2+}$ interactions was observed for both metastable phases. Various scenarios for different motional processes as temperature is increased are discussed.

